



OPEN ACCESS

EDITED BY Giampiero Bardella, Sapienza University of Rome, Italy

REVIEWED BY Surabhi Ramawat. Sapienza University of Rome, Italy Xiaowei Che. Shandong Normal University, China

*CORRESPONDENCE Dipanjan Roy ☑ droy@iitj.ac.in Arpan Banerjee □ arpan@nbrc.ac.in

RECEIVED 06 June 2025 ACCEPTED 25 August 2025 PUBLISHED 10 September 2025

CITATION

Narvaria AS, Banerjee A and Roy D (2025) Neural signatures of prioritization and facilitation in retrieving repeated items in visual working memory Front. Hum. Neurosci. 19:1642615. doi: 10.3389/fnhum.2025.1642615

COPYRIGHT

© 2025 Narvaria, Banerjee and Roy. This is an open-access article distributed under the terms of the Creative Commons Attribution License (CC BY). The use, distribution or reproduction in other forums is permitted. provided the original author(s) and the copyright owner(s) are credited and that the original publication in this journal is cited, in accordance with accepted academic practice. No use, distribution or reproduction is permitted which does not comply with these terms.

Neural signatures of prioritization and facilitation in retrieving repeated items in visual working memory

Abhishek Singh Narvaria¹, Arpan Banerjee^{1*} and Dipanjan Roy^{1,2}*

¹Cognitive Brain Dynamics Lab, National Brain Research Centre NH-8, Gurugram, India, ²Centre for Brain Science and Applications, School of Artificial Intelligence and Data Science, Indian Institute of Technology, Jodhpur, India

Visual working memory (VWM) is a limited-capacity system where working memory items compete for retrieval. Some items are maintained in the working memory in the "region of direct access," which holds information readily available for processing, while other items are in a passive or activated longterm memory state and require cognitive control. Moreover, their recognition requires moving from the most active template in VWM to another one with the shift of attention. Stimulus properties based on similarity can link items together, which can facilitate their retrieval due to prioritization. To investigate the neural dynamics of differential processing of repeated versus not-repeated items in working memory, we designed a modified Sternberg task for testing recognition in a VWM-based EEG study where human participants respond to a probe for an item's presence or absence in the representation of an encoded memory array containing repeated and not repeated items. Significantly slower response times and comparatively poor accuracy for recognizing not-repeated items suggest that they are not prioritized. We identified specific differences in spectral perturbations for sensor clusters in the power of different frequency bands as the neural correlate of probe matching for not-repeated vs. repeated conditions, reflecting biased access to VWM items. For not-repeated item probe matching, delay in beta desynchronization suggests poor memory-guided action selection behavior. An increase in frontal theta and parietal alpha power demonstrated a demand for stronger cognitive control for retrieving items for not-repeated probe matching by shielding them from distracting repeated items. In summary, our study provides crucial empirical evidence of facilitation and prioritization of repeated items over non-repeated items and explains the probable role of different EEG rhythms in facilitated recognition of repeated items over goal-relevant, not-repeated items in VWM.

visual working memory (VWM), repeated items, not-repeated items, prioritization, facilitation, EEG, spectral perturbations

1 Introduction

Working memory refers to our innate cognitive ability to temporarily hold and manipulate relevant information "in mind." Two key features of working memory are its flexibility and its starkly limited capacity to maintain only a limited number of items (Adam and Serences, 2019). In working memory (WM), items are held as mental representations that compete for retrieval, especially during probe comparison tasks. This competition for retrieval can impact how well we remember these items. For example, in a working memory recognition task, non-target items similar to the target create competition and interference. This competition can affect the speed and accuracy of retrieval (Olivers et al., 2011). In such tasks, an attentional template of the probe is created and is compared with different WM representations one after the other in a serial manner and requires attention to bring one representation at a time into an active state in working memory. This process continues till the item matching is completed. As per embedded processing models of working memory (Cowan, 1999; Oberauer, 2002), the items in WM are maintained in focus of attention as in the active state, while less relevant items are in the activated region of long-term memory and are considered to be in a passive state (Larocque et al., 2014; Peters et al., 2009; Li et al., 2020, 2021; Zhang et al., 2022). These states determine how easily accessible these WM representations are during a memory retrieval task.

Prioritization and facilitation of items ease out this competition for retrieval. Items in the form of memorized arrays might lead to enhanced facilitation of WM representations due to perceptual features like their size or hue (Constant and Liesefeld, 2021). This can be due to different mechanisms, which are mainly bottom-up. Regarding multi-item WM retrieval, shared inter-item properties like similarity or repetition of items (Ren et al., 2023; Hamblin-Frohman et al., 2023; Lin and Luck, 2009) can be facilitated. These inter-item properties can lead to repetition facilitation, where these items are bound together in the form of chunks, leading to enhancement in retrieval (Chekaf et al., 2016; Thalmann et al., 2019).

However, this item association is not always facilitatory and can lead to repetition inhibition, as this pattern of similarity or repetition needs to be detected and should not have any lag or be presented very distant from each other (Crowder, 1968; Lee, 1976). This way, WM items do not undergo Gestalt perception (Peterson and Berryhill, 2013). The failure to detect repetition leads to even inhibition as shown in the Ranschburg effect in shortterm memory (Greene, 1991). However, if the pattern is detected, the items bound are chunked, and associative-linked memory items are automatically activated (Oberauer and Lange, 2009). The representation of identical items might lead to a lower activation threshold for their probe matching compared to non-facilitated items (Ren et al., 2023). Hence, these mechanisms are important to answer the question whether repetition of items in a working memory array can lead to better recognition and facilitation of their representations in a probe comparison task, and leads to conflict for non-facilitated items that are not repeated.

In line with the above, one testable hypothesis could be that repeated items (Rep) might be facilitated and interfere with probe matching for not-repeated items (NRep) in VWM, impacting their retrieval during working memory performance. Moreover, the competition for facilitated retrieval might depend on the role of attention in inhibiting irrelevant representations and response preparation in VWM. The probe matching for VWM representations must be reflected in the EEG data based on the alteration in brain oscillations and may shed crucial insight into their possible neural correlates for prioritization, facilitation, or hindrance in the VWM recognition task.

The probe matching window is important because it allows researchers to isolate the neural activity associated with matching a new input (the probe) with stored information in visual working memory (VWM). Different frequency bands, like alpha, theta, and beta, reflect different cognitive processes involved in this matching, including allocation of attention, memory maintenance, and conflict in decision making. The changes in frequency bands during the probe matching window provide critical insights into how attention is allocated to the matching probe, which is required for matching the attentional template to maintained VWM representations. During VWM, the dynamics of neural beta (13-30 Hz), especially in the central electrode, are associated with memory-guided behavior as it can affect motor preparation, as shown by previous studies (Boettcher et al., 2021; Nasrawi et al., 2023; Nasrawi and van Ede, 2022; Schneider et al., 2017). Such motor preparation signals index the access to items to be prioritized within VWM (Ding et al., 2024). Extant literature further suggests that the Alpha frequency band plays a crucial role in sensory information-specific attention requirements. Interestingly, changes in the relative priority of stored representations and maintenance are reflected in the modulation of posterior alpha power oscillations (8-14 Hz) as reflected in alpha lateralization for the selection of task-relevant information for the internal selection of information maintained within VWM (van Ede et al., 2017). Increase in alpha power is related to active inhibition of task irrelevant items (Benedek et al., 2014).

Complex behavioral tasks require a higher need for cognitive effort and conflict monitoring (Cavanagh and Frank, 2014; Cavanagh and Shackman, 2015; Cavanagh et al., 2012). In line with this, previous studies have reported Theta power (4–7 Hz) oscillatory changes related to top-down control over items (Sauseng et al., 2010; Sauseng and Liesefeld, 2020). More specifically, it has been shown that the frontal theta controls the endogenous attentional selection mechanisms of task-relevant items (Johnson et al., 2017; Sauseng et al., 2010). Alteration in the power of Fronto-medial theta can resolve the conflict in probe matching for irrelevant items in the probe conditions.

In this study, to capture the bias in probe matching for repeated vs. not-repeated items in the VWM task and its neural correlates, we have conducted an EEG study that utilizes a memory array facilitating the encoding of items of both the repeated and not-repeated categories. The encoding of items of both categories with an equal chance of the appearance of a relevant probe. This is to gain empirical evidence for how WM representation of certain WM items is prioritized and behaviorally influences facilitation for repeated or not-repeated items as captured by individual response time and accuracy for responding to relevant probes. Next, we investigate their neural correlates using EEG to test our hypothesis that band-specific spectral power differences in theta and alpha across two conditions (repeated and not-repeated) reveal attentional facilitation of certain items, which lead to conflict in probe matching for those items which are not facilitated during

memory retrieval and can be associated with underlying causes for task-specific behavioral differences elicited by the participants.

2 Materials and methods

2.1 Participants

Data from an earlier conducted pilot study (N = 7)where following were the group means of two conditions $M_{Rep} = 669.76 \text{ ms} \text{ (SD = 202.16 ms)} \text{ and } M_{Nrep} = 741.78 \text{ ms}$ (SD = 262.15). These data gave an observed effect size of d = 0.68as calculated via G*Power's effect size calculator (Faul et al., 2007). With $\alpha = 0.05$ and desired power = 0.80 (two-tailed test) for t-test family indicated that a minimum of sample size of 20 participant would be needed. Multiple relevant studies including (Ren et al., 2023; Hamblin-Frohman et al., 2023; Lin and Luck, 2009) on prioritization in working memory task due to similarity and identicality have a sample size of at least 22. Twenty-five participants (12 females; M(age) = 25.04 years, SD = 2.52 years, range: 21-32 years) were recruited for the study. All participants had a university degree or higher, were right-handed, reported normal or corrected-to-normal vision, and declared no history of neurological or psychiatric disorders. Two participants' data were not included in the analyses as one did not follow the proper instructions, and the other performed below the chance level in behavioral analysis of accuracy. Following this, data from a total of 23 participants (11 females; M(age) = 24.82 years, SD = 2.12 years, range: 21-28 years) were included in the present study for further analysis.

2.2 Ethics statement

The study was carried out following the ethical guidelines and prior approval of the Institutional Human Ethics Committee (IHEC). Written informed consent was obtained from all participants before the commencement of the experiment, and they were remunerated for the time of their participation.

2.3 Stimuli and trials

The working memory task for the study was designed and presented using Presentation® software (Version 23.0, Neurobehavioral Systems, Inc., Berkeley, CA) and displayed on a 22-inch LED monitor screen (60 Hz; 1920×1080 pixels) at a viewing distance of approximately 75 cm.

In both the main experiment and practice trials, visual working memory was tested using a probe-matching task (Figure 1). Participants were subjected to 280 trials in 6 blocks, with each block lasting 7–8 min and a break of around 2 min. Participants responded in a two-alternate forced-choice (2-AFC) manner using the left and right arrow keys of the keyboard for "No" and "Yes," respectively.

2.3.1 Memory array

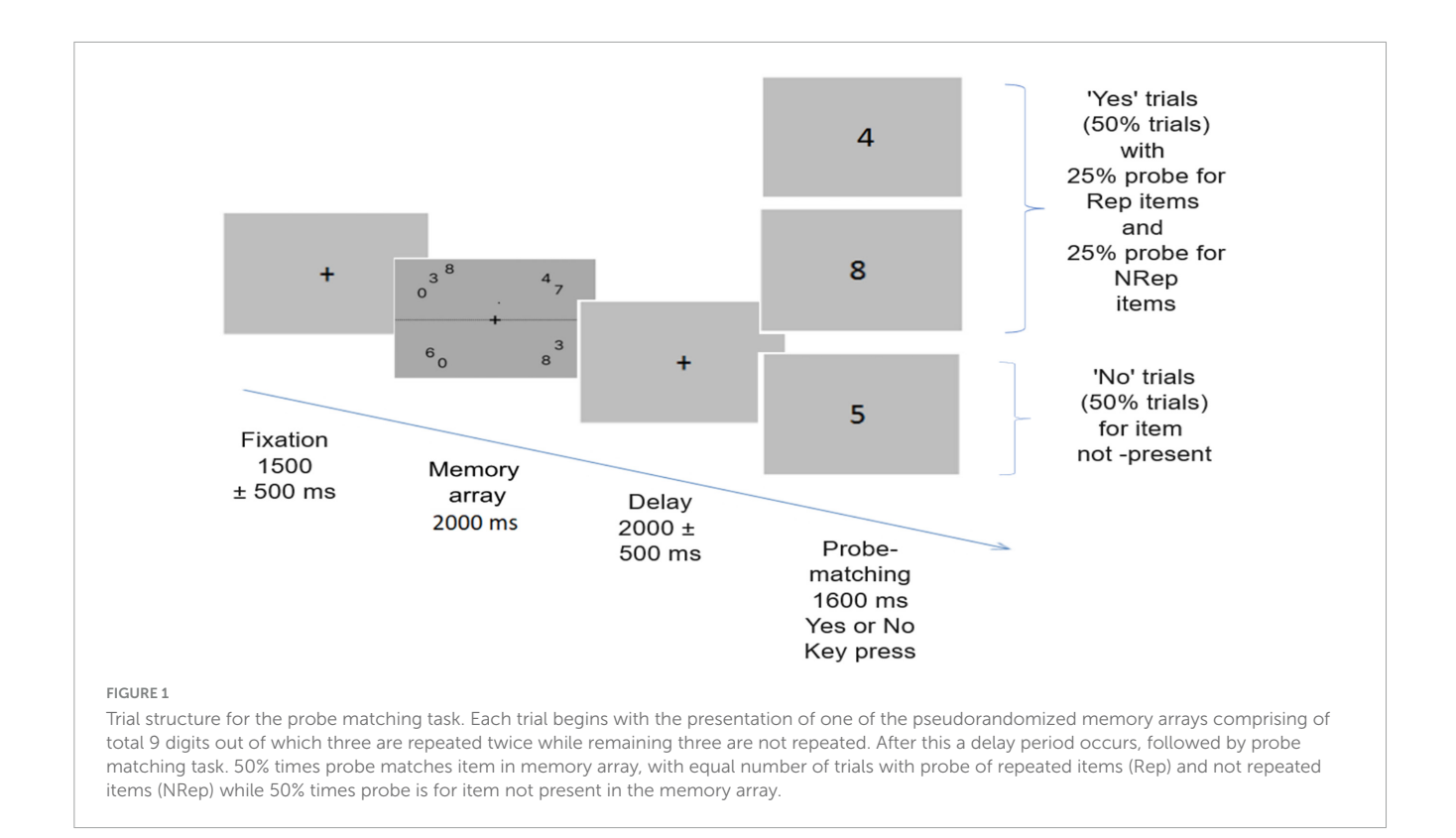
The memory array comprises of stimuli set where nine number digits were shown in each memory array, out of which three items were repeated twice and arranged in a jumbled fashion, along with three items that were not repeated; in total, nine items were presented in each memory array arranged in a circular fashion around fixation cross. These nine items are displayed with two to three items randomly shuffled between each quadrant to avoid encoding bias. Our rationale was to fully utilize the working memory capacity of 7 plus or minus 2 (Miller, 1956) and facilitate the formation of chunks (Cowan, 2010). Furthermore, sets of numbers used in a particular array were controlled to prevent the formation of commonly used chunks (e.g., numerical order, odd or even set, etc.). Numbers were shown within the foveal area (dva < 2.5 degrees), and each item subtends an angle of 0.76 degrees. Hence, all memory arrays were presented as stimulus images during the trials and were pseudo-randomized. Memory arrays were shown for 2000 msec on average.

2.3.2 Trial structure

After presenting a black fixation cross for 1500 \pm 500 msec, a memory array appeared for 2000 msec, which participants were instructed to remember. After the presentation of the memory array, a delay screen appears for 2000 \pm 500 msec with a cross in the centre, followed by the onset of the probe on which participants had to respond whether the probe item was present in the memory array or not by using the left and right arrow keys. A black fixation cross was presented on a dark gray background throughout the trial. Participants were instructed to give responses as fast and accurately as possible. Response time and accuracy were estimated from behavioral data. The inter-trial interval (ITI) appears as a black screen after a response window of 1600 msec. Out of the total 280 trials, 140 were "No" trials in which participants had to respond to a probe for which item was not present in the memory array. The remaining 140 "Yes" trials were for probes having a corresponding item in the memory arrays. Out of all the "Yes" trials, half had a probe for Rep items, and the other half had a probe for NRep items.

2.4 Behavioral analysis

Next, the response time and accuracy in the memory task were quantified for each participant. For response time and accuracy analysis, we used data from all the "Yes" trials of the Repeated (Rep) and Not-Repeated (NRep) categories, where response time and accuracy were calculated for the response window starting from probe onset till button press for Yes or No for probe matching. Data from two subjects were not included in the analysis, as one subject had poor accuracy (38%), whereas the other participant did not follow the instructions well. Outlier trials were removed using the Inter-Quartile range (IQR) method, where any data point less than 1.5 times the IQR below the quartile (Q1) or greater than 1.5 times the IQR above the quartile (Q3) is removed. Only trials with correct responses for probe matching in Rep and NRep conditions were used for response time analysis. After removing the outlier trials, response accuracy was analyzed. Two-tailed Wilcoxon signed-rank test was used to compare for significant differences in response time and response accuracy for Rep and NRep conditions. Effect size was



quantified using r (the value of the z-statistic returned by the test, divided by the square root of the sample size). The "No trials" were introduced to balance the probe probability for Rep and NRep trials and to avoid the guessing for "Yes trials." They were not comparable to our study conditions and were excluded in the further analyses.

2.5 Data acquisition and analysis

2.5.1 EEG data

EEG recordings were obtained from 64 Ag/AgCl active electrodes (Brain Products GmbH, Gilching, Germany) using a Brain Vision Recorder. The 64-channel EEG signals were recorded using the International 10% electrode placement system and checked before and after the experiment. Reference electrodes were Cz, grounded to AFz. Channel impedances were kept at $<\!25~\mathrm{k}\Omega$. Data were acquired continuously with sampling rate of 1 kHz.

2.5.2 Pre-processing for EEG signals

Analysis was conducted on twenty-two participants' EEG data using MATLAB® and the EEGLAB toolbox (Delorme and Makeig, 2004). Data of one participant was discarded at this step due to very noisy recordings (with asymmetric variations of very large amplitudes due to a skull implant that the participant informed later). EEG data were down-sampled to 256 Hz, and High-pass (0.5 Hz) and low-pass filters (45 Hz, respectively) were applied before the data were re-referenced to the linked mastoid (TP9 and TP10). Noisy channels were removed after visualization of spectral power over those channels and removal of bad temporal segments. Next, we applied the Infomax independent component analysis (ICA) algorithm to detect artifactual ICAs (eye blinks, ocular, muscular, and electrocardiograph artifacts), and subsequently,

these components were removed manually after visual inspection. Epochs of 0–1600 msec were extracted from the probe display onset till the end of the response window. They were sorted for the Rep and NRep two probe conditions and used for the Eventrelated spectral perturbation (ERSP) analysis. ERSP was computed using the newtimef function of the EEGLAB toolbox. The data was decomposed in a time-frequency domain across a frequency range from 3 to 30 Hz using a complex Morlet wavelet. The preprobe duration (-1000 to 0 ms) was used as a baseline for baseline subtraction.

2.6 Spectral analysis

The pre-processed EEG data was decomposed in a timefrequency domain across a frequency range from 3 to 30 Hz using function newtimef in EEGLAB and is computed by convolving three-cycle complex Morlet wavelets. These analyses were based on 200-time points from -1000 to 1600 msec, centered on the appearance of the probe till the end of the response time window, for the epoch corresponding to probe absence/presence, the number of cycles in the wavelet increased linearly from 2 (at 3 Hz) to 18 (at 30 Hz). The wavelet used to measure the amount and phase of the data in each successive, overlapping time window begin with a 3-cycle wavelet (with a Hanning-tapered window applied) and '0.8' is the number of cycles in the wavelets used for higher frequencies will continue to expand slowly, reaching 20% (1 minus 0.8) of the number of cycles in the equivalent FFT window at its highest frequency. The resulting temporal window ranged from approximately 666 ms at 3 Hz to 600 ms at 30 Hz. Power values (in dB) were baseline-corrected by subtracting the mean power in the time window before the presentation of the probe

(-1000 to 0 msec) from the power in the post-probe onset window. This pre- probe window was chosen for better temporal accuracy and contextual matching to avoid unneccessary fluctuations and capturing the relevant brain states. The ERSP was obtained by averaging the normalized representations across epochs, separately for the two probe conditions Rep and NRep. Epochs were baseline corrected by removing the temporal mean of the EEG signal on an epoch-by-epoch basis. Only trials where participants responded correctly to the probe were included in these analyses to observe the difference between probe matching for Rep and NRep categories.

2.7 Electrode selection

To explore the beta band ERSP dynamics at (13–20 Hz) we focused our analyses on C3 electrode which was contralateral to the tight hand required for correctly responding to presence of "Yes" trials irrespective of spatial position of relevant item in the stimuli array. The amount of beta desynchronization and temporal lag in beta power is a well-established neural marker of manual action planning (Baker, 2007; Ding et al., 2024; McFarland et al., 2000; Neuper et al., 2006; Van Wijk et al., 2009). To study role of frontal medial theta band oscillations (Ferreira et al., 2019; Onton et al., 2005; Sauseng et al., 2010) between 4 and 8 Hz following electrodes were selected F1, F2, Fz, FCz, FC1, FC2, C1, and C2. Frontal-midline electrodes have been shown to involve theta oscillations with relation to probe evaluation and response conflict (Cavanagh and Frank, 2014; Sauseng et al., 2005).

2.8 Statistical analyses of ERSP power changes

In the time-frequency analysis, we used the cluster-based permutation statistics to test for statistically significant differences in ERSP power for two probe-matching conditions (Rep and NRep) using EEGLAB's toolbox's statcond function along with false discovery rate (FDR) correction for multiple comparisons to estimate time-frequency clusters that were significantly different (with p < 0.05) between Rep and NRep conditions for the period around probe appearance till the end of the trial at 1600 msec (Maris and Oostenveld, 2007). Here, the null distribution is created by repeatedly shuffling the condition labels and recalculating the test statistic under the assumption of no true difference between conditions. The null distribution generated was used to compare the observed data clusters, which were considered significant if their difference exceeded the 95th percentile of the null distribution (p < 0.05, two-tailed). In addition, we visualized scalp maps for which ERSP values were averaged for different frequency bands for Rep and NRep conditions. The time period and frequency range for sensor analysis were decided based on identified significant clusters using time-frequency analyses and generated plots. We used cluster-based permutation statistics with 2000 iterations to identify sensors with statistically significant differences in ERSP power for the two conditions for all of our analyses using statcond function in the EEGLAB toolbox. Two-tailed paired t-tests with a false positive (alpha) threshold of 0.05 were used to identify significant clusters, along with permutation statistics, and to evaluate the sensors exhibiting statistically significant differences in ERSP power. Statistically significant clusters exceeded the 95th percentile of this null distribution. The details of all the specific individual analyses are further elaborated in the results section. Statistical analysis was carried out separately for alpha (8–12 Hz), theta (4–7 Hz), and beta (13–30 Hz) frequency ranges.

2.9 Correlational analysis between response times (RTs) and peak desynchronization time

We performed a trial-wise correlation analysis between response time (RT) and the latency of peak beta desynchronization in the post-probe window to examine the relationship between neural timing and behavioral responses. Time-frequency data were extracted for the beta band (13-20 Hz) at the C3 electrode, and peak desynchronization latency was defined as the time point with minimum beta power within each trial, reflecting maximal suppression. Trials were grouped according to experimental conditions, Rep and NRep. RTs were obtained from their event markers in EEG data. Trials were excluded if they exhibited extreme RTs (<150 ms or >1000 ms) as beta desynchronization never happens before 200 ms or after 1000 msec (Kilavik et al., 2013; Makeig, 1993; Pfurtscheller and Da Silva, 1999). Trials with RT or desynchronization time outside the 2.5th-97.5th percentile range were excluded as Outliers. We used Spearman's rank correlation to assess the monotonic relationship between RT and desynchronization timing for the two conditions separately, due to deviation from norma distribution of the raw values. The correlation was calculated across trials using a two-tailed significance threshold of $\alpha = 0.05$.

In addition, effect sizes for the difference in Response times (RTs) and in beta desynchronization latency between the two experimental conditions (Rep vs. NRep) were calculated for the C3 electrode using Cohen's d for paired samples. This provided a standardized measure of the magnitude of condition-related changes.

2.10 Data and code accessibility

All the behavioral and EEG data acquired from the participants and the analysis carried out during this study are available from the corresponding authors upon reasonable request. The pre-processed EEG data and codes/scripts used for all the analyses conducted in this paper will be made freely available to download from https://github.com/dynamicdip/.

3 Results

3.1 Behavioral response

We only used data for trials with correct responses for probe matching in Rep and NRep conditions in the response time analysis. The violin plots (Figure 2A) (generated using ggplot2

(Wickham, 2011) in R software) for both conditions depict that the response times for probe matching follow Rep < NRep. The Response time distribution of the Rep condition is skewed and visually asymmetric. Hence, we employed a non-parametric two-tailed Wilcoxon signed-rank test to compute the statistical significance of differences between the medians of response times (RTs) of any two categories. Effect size was quantified using r (the value of the z-statistic returned by the test, divided by the square root of the sample size). We rejected the null hypothesis as we found using the Wilcoxon Signed-Rank test that there is a statistically significant difference between Rep and NRep with Rep having lower RT values (Median = 677.5, n = 25) than NRep (Median = 741.1, n = 25), (Z = 4.3589, p < 0.001, r = 0.87).

For response accuracy analysis, mean percentage accuracy (MPA) was calculated and plotted (Figure 2B) with distinguishable differences in distribution and median values of response accuracy using the two-tailed Wilcoxon Signed-Rank test. Effect size was quantified using r (the value of the z-statistic returned by the test, divided by the square root of the sample size). This Wilcoxon Signed-Rank test showed that response accuracy was significantly higher for the matching probe for Rep items (median = 100, n = 25) in comparison to that for NRep items (Median = 80, n = 25) with Z = -4.3589, p < 0.001, r = -0.87.

3.2 Event-related spectral perturbations in Rep versus NRep probe conditions

Next, we characterized whether the neural dynamics might reflect changes in spectral perturbations in different frequency bands due to these differences in response time and accuracy for the two probe-matching conditions.

In Figure 3A, ERSP with data for both Rep and NRep conditions collapsed into one plot to visualize the grand average ERSP across all the electrodes for values for frequencies ranging from 3 to 30 Hz and for the temporal duration of -100 to 1100 msec post-probe presentation for ERSP plots, where 0 msec represents the onset of the probe across all subjects. This was done to avoid circularity in Time of interest (TOI) selection for analysis; instead, peak values of different EEG oscillatory rhythms are utilized based on data visualization. No statistical tests were performed at this level. Alpha was most prominently desynchronized between 400 and 800 msec at 9–12 Hz. Also, event-related desynchronization was visible in the beta band between 13 and 21 Hz around the temporal window of 300–650 msec. The synchronization of the theta band is visible in the range of 4–7 Hz around the temporal window of 100–500 msec.

3.3 Topographical difference in parieto-occipital alpha power

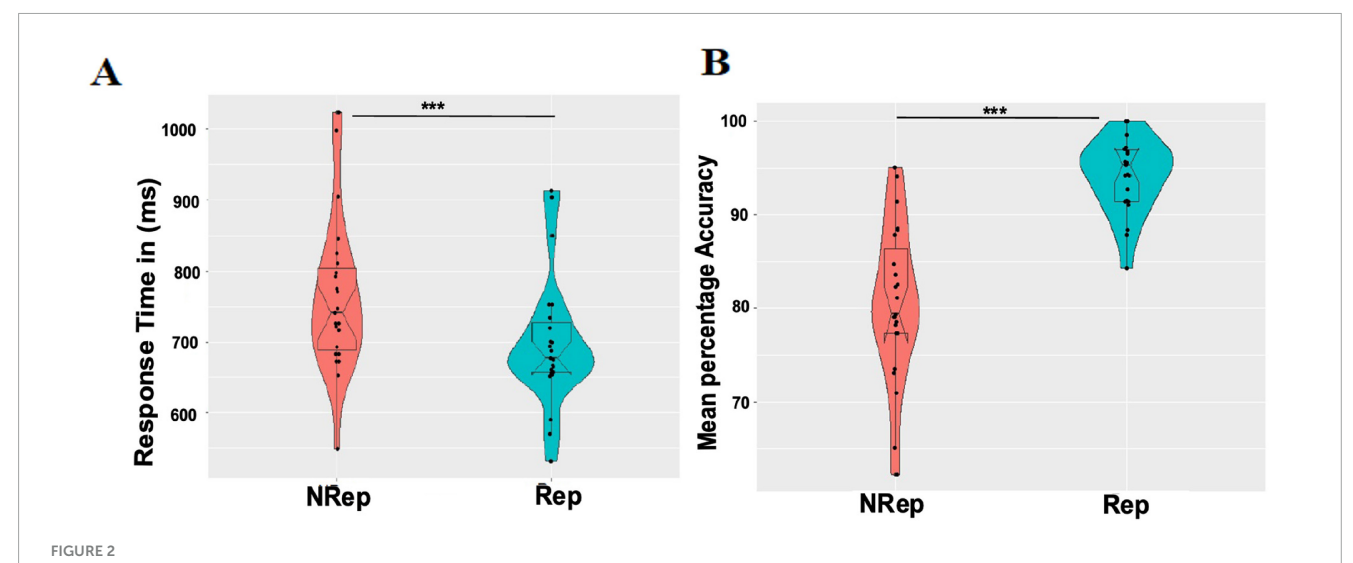
Attention typically plays an important role in VWM retrieval; hence, we were interested in studying the role of the alpha band oscillations in mediating internal attention and suppressing irrelevant representation in WM during probe matching. Event-related alpha desynchronization was observed as depicted in Figures 3B, C. Furthermore, Figure 3C shows relatively increased

alpha power in the right parieto-occipital area for NRep in comparison to Rep conditions as displayed in Figure 3B. The topoplots generated (Figures 3B–D) using cluster-based permutation statistics in the relevant temporal response window of 400–800 msec after probe onset and in the range of 9–12 Hz frequency revealed significant involvement of parieto-occipital electrodes namely PO8, P4, and P8, showing enhanced power change in NRep compared to Rep conditions. We observed one negative cluster consisting of right parietal sensors, namely PO8, P4, and P8 [$t_{(21)} = -2.97, p < 0.001$], with t-value peaking at -3.35 for PO8.

3.4 ERSP difference in beta power for Rep vs. NRep probes

Next, we investigated beta band (13–20 Hz) desynchronization in C3, i.e., contralateral, which may be responsible for the response by the right hand with "Yes" for valid probe-matching, which indexes the prioritization of item in retrieval by enhancing the motor preparation for appropriate response selection in VWM for two conditions.

Figures 4A-C display ERSP plots for the C3 electrode averaged over frequency from 13 to 20 Hz separately for each condition from -100 to 1100 msec around probe onset. Cluster-based permutation analysis revealed a significant (negative) cluster in beta band (13-20 Hz) between 200 and 400 ms post-probe presentation over C3 electrodes with $[t_{(21)} = -176.91, p = 0.018]$ peaking at 350 ms and 16.5 Hz, showing faster desynchronization in beta band for Rep condition compared to NRep condition. NRep condition (Figure 4B) indicates relatively delayed desynchronization of the beta band for the NRep compared to the Rep condition. In the Figure 4D, condition-wise modulations are visualized in the beta band, from the ERSP power which was averaged across subjects was extracted for the electrode C3 in the 13-20 Hz range to obtain line plots. Mean ERSP beta power for the two conditions were plotted with time (-300 to post-stimulus) on the x-axis and power (in dB) on the y-axis. Peak desynchronization time with most negative ERSP power was identified for Rep and NRep. Both the conditions showed a clear desynchronization following the probe onset at electrode C3. Rep condition reached peak desynchronization at 406 ms at -2.26 dB (in red dashed line), whereas NRep showed a slightly delayed desynchronization at 480 ms at -2.33 dB (in blue dashed line). Shaded areas around each line indicates \pm 1 standard error of the mean (SEM) across participants. No statistical test was applied here. Then we did Spearman's correlation analyses, which revealed a significant but very weak positive correlation between the latency of peak beta desynchronization and RT for NRep. whereas Rep showed no significant correlation. For Rep, Spearman r = 0.05, p = 0.1910 (N = 578 trials) while for NRep condition, Spearman's r = 0.14, p = 0.002 (N = 452 trials). In Figure 4E, scatter plots with regression lines shows significant correlation for NRep but not for Rep condition. The 95% confidence interval for the fitted regression line is shown with shaded area. The difference in Response times (RTs) and peak beta desynchronization latency between the Rep and NRep conditions yielded a Cohen's d of -0.94 and -0.18, respectively, corresponding to a large effect size for RTs but a very weak effect size for peak betra desynchronization latency.



Behavioral results. (A) Each violin plot shows responses time distribution for each condition (NRep Vs Rep). Each dot represents average response time for one participant. (B) Mean percentage accuracy distribution for each condition (NRep Vs Rep) where each dot represents average accuracy (in percentage) for one participant. ***p < 0.001.

3.5 ERSP differences frontal-medial theta band oscillations

Next, we investigated the frontal-medial electrodes involving multiple sensors F1, F2, Fz, FCz, FC1, FC2, C1, and C2. To examine the difference in theta power for the two probe conditions. Using cluster-based permutation, we found significant negative cluster at around 5-7 Hz and 600-900 msec even after FDR correction with $[t_{(21)} = -561.22, p = 0.022]$ peaking at 800 ms and 6.5 Hz, reflecting significantly higher theta power with a threshold of 0.05 for retrieving items using the probe for NRep category in ERSP plot (Figures 5A–C). The topographical distribution of ERSP (Figures 5D-F) over fronto-medial electrodes involving multiple sensors F1, F2, Fz, FCz, FC1, FC2, C1, and C2. The selection of these sensors was motivated by the previous studies (Ferreira et al., 2019). In particular, C1 and C2 electrodes were used for analysis in place of Cz, as it was used as the reference electrode. The cluster of these sensors was depicted in Figures 5D-F, where permutationbased analysis was done for 5 to 7 Hz and a period of 600-900 msec after probe onset. Multiple sensors, namely Fz, FC1, FC2, C1, C2, F1, and FCz, showed significant negative clusters in average ERSP power with $t_{(21)} = -16.04$, p < 0.02, with *t*-value peaking at -2.66for FC1, showing an increase in average ERSP power for the NRep condition over the Rep condition.

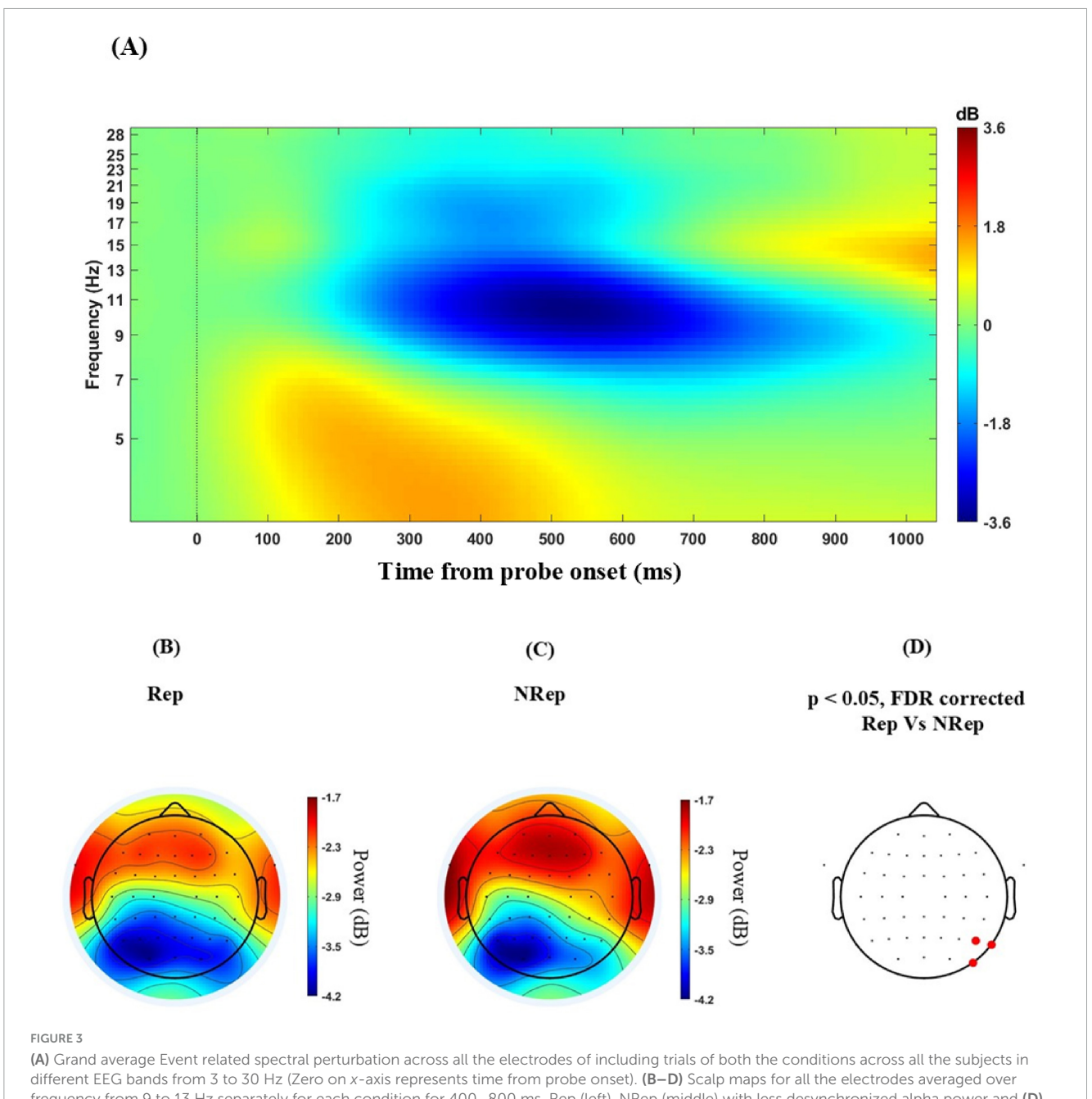
4 Discussion

The present study investigated the difference in probe comparison in a VWM task across two conditions, Rep and NRep. Here, the difference in behavior was empirically studied in terms of response time and accuracy for matching the relevant probe. Probes were matched with the maintained WM representations, where the probe acts as an attentional template to match with the relevant representation one at a time until its match is found (Woodman et al., 2007). The

most facilitated representations are in direct access (Oberauer, 2002), while other representations are brought into focus of attention sequentially. Subsequently, using ERSP analysis, we investigated how spectral perturbations of different brain oscillations differ in probe matching for the two probe conditions, Rep and NRep. Different brain oscillations provide further evidence for this bias in processing different items in the WM task.

Behavioral results showed that Rep items probes match faster and more accurately to relevant representations in comparison to the NRep probes. Our results provide evidences for the facilitation of Rep representations in probe matching, comparable to that of visual similarity in the working memory paradigm (Hamblin-Frohman et al., 2023), but by using the repetition of numbers as a linking feature between items (Oberauer and Lange, 2009). Our experimental results demonstrate that the default prioritization of representations of Rep items is a feasible scenario in response selection, as they are facilitated during maintenance and when they are retrieved for valid probe matching (van Moorselaar et al., 2014).

Contrary to the bottom-up saliency view (Theeuwes, 1992; Wolfe, 1994), which suggests that non-redundant dissimilar items should have gained prioritized access in VWM, as also seen in the Ranschburg effect (Crowder, 1968), we found that repeated items were facilitated during VWM retrieval, reflecting an enhanced and stable representation of repeated items in VWM (Ren et al., 2023). One probable reason for such attentional facilitation is the chunking strategy for repeated items (Thalmann et al., 2019), leading to the prioritization of repeated items over the not-repeated items as fewer slots are required, also resulting in freeing up space to accommodate more items (Chekaf et al., 2016). In the imagined visual space, the chunks of repeated items take up less space for number of items. This finding further implies that probe matching for repeated items requires less effort as their representation were in an active state for direct access (Chekaf et al., 2016). This further suggests the internal representation of attentionally prioritized Rep items might conflict with valid probe matching for NRep

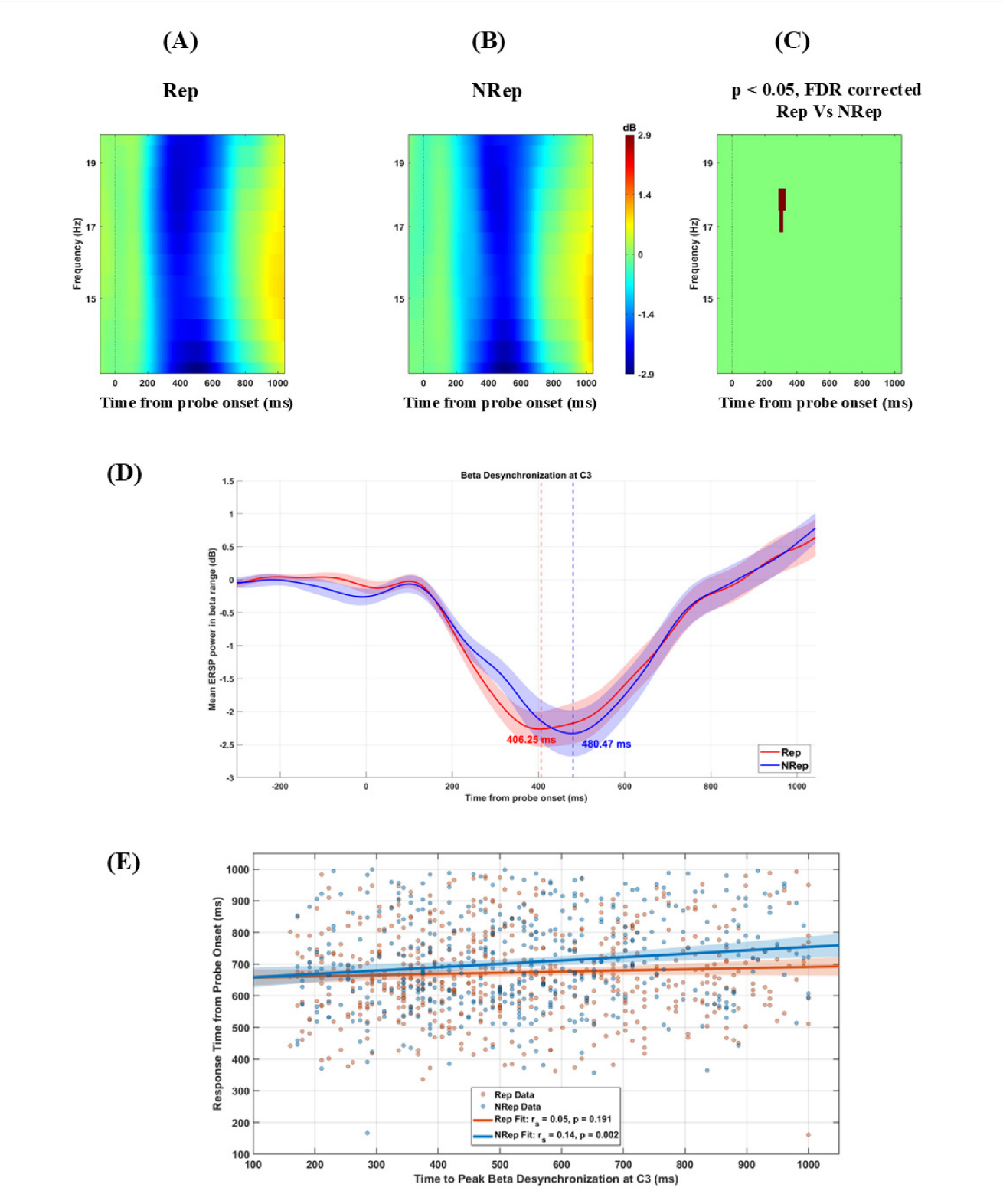


(A) Grand average Event related spectral perturbation across all the electrodes of including trials of both the conditions across all the subjects in different EEG bands from 3 to 30 Hz (Zero on x-axis represents time from probe onset). (B-D) Scalp maps for all the electrodes averaged over frequency from 9 to 13 Hz separately for each condition for 400-800 ms. Rep (left), NRep (middle) with less desynchronized alpha power and (D) show a plot of FDR-corrected clusters with the threshold of 0.05 reflected on the vertical bar after cluster-based permutation showing a significant difference (red dotted) in PO8, P4 and P8 for ERSP-based topographies of two conditions for right parietal electrodes.

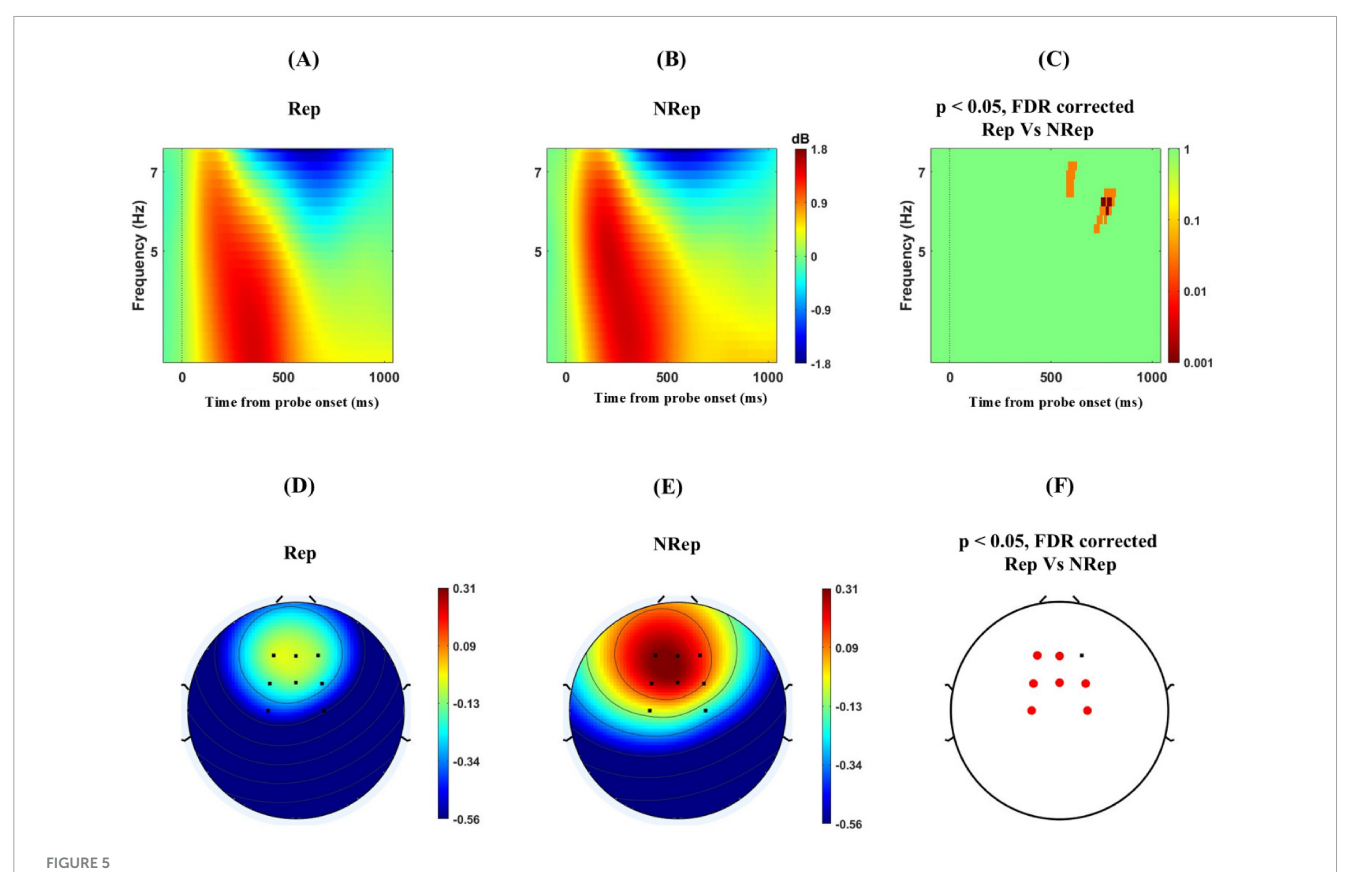
items, which require flexible allocation of attention to NRep items (Emrich et al., 2017).

Our ERSP results further revealed the role of different frequency bands in differential response selection, attentional demands, and conflict in decision making, which are required for probe matching of Rep and NRep probes in VWM. Beta power is mostly attributed to its role in sensory-motor function involving motor response selection, where it has been found to index the prioritization of items in VWM (Ding et al., 2024). Here, we predicted that the attentional template for Rep items' representations is prioritized in the maintained WM, which facilitates WM recognition during valid probe matching. In this

study, we find that the Beta band (13–20 Hz) in the C3 electrode is desynchronized early at around 200 ms, shortly after probe presentation for repeated items and is significantly different in ERSP power for Rep vs. NRep conditions, which facilitates the right hand's key press for valid probe matching and might be associated with faster and clearer motor preparation for response selection as also suggested by shorter response time and high accuracy for Rep over NRep in the behavioral results possibly due to repetition of items, also related to facilitation of identical objects in VWM (Ren et al., 2023). Delayed beta desynchronization was observed for the NRep condition in the line plot compared to Rep which suggests that when the attentional template tries to match NRep



Beta power change for the two conditions. (A–C) display ERSP plots for C3 electrode averaged over frequency from 13 to 20 Hz separately for each condition from -100 to 1100 msec (Zero on x-axis represents time from probe onset). Rep (left), NRep (middle), and plot of FDR corrected clusters with the threshold of 0.05 after cluster-based permutation (right) showing significant difference in ERSP of two conditions. NRep condition shows positive cluster with delayed desynchronization of beta band here in comparison to Rep. (D) Mean ERSP time series (13-20 Hz) at electrode C3 for both conditions (N = 22). Rep and NRep show beta desynchronization following probe onset (0 ms). Vertical dashed lines indicate peak desynchronization time points for each condition. Rep condition reached peak desynchronization at 406 ms at -2.26 dB (in red dashed line), whereas NRep showed a slightly delayed desynchronization at 480 ms at -2.33 dB (in blue dashed line). (E) Scatterplot showing trial-wise correlation between peak beta desynchronization latency (ms) and response time (ms) at C3 electrode for conditions Rep and NRep. Regression lines are shown. A significant positive correlation was observed only for NRep condition (Spearman's r = 0.14; p < 0.01). The 95% confidence interval for the fitted regression line is shown with shaded area.



Increased Frontal—medial theta (FMT) power for responding for NRep items in comparison to Rep items. (A—C) shows ERSP plots with positive clusters averaged over frequency from 4 to 7 Hz separately for each condition for a period of –100 to 1100 msec for frontal-medial electrodes namely involving multiple sensors F1, F2, Fz, FCz, FC1, FC2, C1, and C2 (Zero on x-axis represents time from probe onset) Rep (left), NRep (middle), and plot of FDR corrected clusters with threshold of 0.05 reflected on the vertical bar after cluster-based permutation (right) showing significant difference in theta power ERSP of two conditions. (D—F) Scalp maps for Fronto-medial electrodes averaged over frequency from 5 to 7 Hz separately for each condition for 600–900 msec. Rep (Left), NRep (middle), and significant FDR corrected clusters in frontal region (red dotted) Fz, FC1, FC2, C1, C2, F1and FCz with the threshold of 0.05 after cluster-based permutation (right) showing significant difference in ERSP based topography of two conditions with increase theta power for NRep.

category, there is a conflict and delay for probe matching. The delayed prioritization in NRep compared to the Rep condition is probably due to the default prioritization of Rep representations. In the Correlational analysis, late peak beta suppression for NRep was weakly associated with longer RTs, suggesting that the timing of beta desynchronization may reflect the neural readiness for motor execution for response. Although the effect size was very small (r = 0.14), such magnitudes are typical for trial wise EEGbehavior correlations, as several other neural processes take place alongside. In order to understand the factors behind this bias in directing attention to probe relevant representations, we studied other ERSP power of other frequency bands. Parieto-occipital alpha has been shown to act as a marker for attention when selecting task-relevant information in the WM paradigms (Ichihara-Takeda et al., 2015; Klimesch, 1999). Active inhibition of non-relevant but distracting repeated item's representations requires attentional suppression during probe matching for not-repeated condition (Carlisle, 2019). This is reflected in the relative increase in alpha power and comparatively reduced alpha desynchronization for parieto-occipital electrodes when matching probe for NRep items compared to Rep. This indicated less efficient active inhibition of items of Rep that need to be inhibited during NRep as shown in previous findings (Benedek et al., 2014; Erickson et al., 2019).

Comparatively increased fronto-medial theta power for responding to probe matching for NRep items implies the role of cognitive effort for valid selection and to resolve the conflict arising from matching the relevant probe. This is in line with conflict in WM retrieval and cognitive effort literature, (Botvinick et al., 2001; Jacobs et al., 2006; Onton et al., 2005; Zuure et al., 2020) where the increase in power of the theta band resolves the conflict arising when the attentional template of a valid NRep probe matches with facilitated Rep representations. Increased theta power during NRep items probe matching appears due to interference by repeated item representations, similar to frontal-medial theta power effects of cognitive interference (modulated by distractor strength) as suggested by Nigbur et al. (2011), Magosso and Borra (2024). Previous research from de Vries et al. (2018), Riddle et al. (2020) supports the crucial causal role of theta in prioritizing task-relevant information and potentially suppressing information that is no longer relevant for successfully guiding behavior. For Rep, Theta power is comparatively lower due to the repetition enhancementlike effect, as the default prioritization of repeated items reduces the effort to retrieve. However, for NRep the frontal medial theta power is higher due to cognitive control demands. Here, we fixed the number of items so that varying working memory capacity does not affect the theta power. In contrast to our expectation,

the difference in ERSP power for parieto-occipital alpha band temporally precedes the frontal-medial theta power change, which means that efficient probe matching requires alpha for template matching, which then is supported by frontal-medial theta for avoiding distraction from irrelevant matching. This relatively enhanced frontal medial theta power for NRep than Rep reflects on its probable role in resolving the conflict in probe matching due to irrelevant items in the probe conditions (Cohen and Donner, 2013; Kaiser et al., 2022).

In summary, our study provides evidence for facilitation and prioritization of repeated items as seen in the behavior for probe matching, where shorter response time and higher accuracy for Rep items creates conflict in processing passively maintained representations of NRep items. This explains that items in VWM are retrieved in an order where prioritized representations are facilitated due to certain perceptual features like repetition, and followed by not-repeated items, which are less facilitated. As repeated items are facilitated, the response time for their selection in the presence of a probe requires the least motor preparations with faster action planning, as can be seen in faster beta band desynchronization. The probe matching for NRep items showed delayed desynchronization of beta at the C3 electrode, which is characteristic of slow response preparation. However, for notrepeated items attention need to shift from the representation of repeated items in presence of relevant probe along with attentional suppression of facilitated repeated items' representations. The increase in parieto-occipital alpha power for NRep contributes to the active inhibition of irrelevant but default-prioritized Rep items during probe matching. Stronger cognitive control is required to maintain the NRep representation, whereas Rep representations distract while generating the relevant motor response. However, the cognitive control demands of probe matching for Rep is less, as it is facilitated due to repetition. Increase in Fronto-Medial theta power suggests a link to resolving the conflict of matching the probe for NRep items over Rep items. These evidences provide an explanation for prioritization and facilitation of the interitem feature of repetition interfering with the items that are not facilitated, even if they are relevant. Taken together, our study provides crucial empirical evidence of facilitation and prioritization of repeated items over non-repeated items and elucidates how different EEG rhythms might facilitate recognition of repeated items over goal-relevant, not-repeated items in VWM.

Data availability statement

The datasets presented in this study can be found in online repositories. The names of the repository/repositories and accession number(s) can be found below: https://github.com/dynamicdip/.

Ethics statement

The studies involving humans were approved by Institutional Human Ethics Committee (IHEC) National Brain Research Centre Manesar. The studies were conducted in accordance with the local legislation and institutional requirements. The participants provided their written informed consent to participate in this study.

Author contributions

AN: Visualization, Formal analysis, Writing – original draft, Data curation, Methodology, Conceptualization, Resources, Writing – review & editing, Validation, Investigation. AB: Supervision, Visualization, Project administration, Funding acquisition, Resources, Validation, Writing – review & editing, Software. DR: Software, Resources, Funding acquisition, Writing – review & editing, Validation, Data curation, Methodology, Supervision, Visualization, Project administration, Conceptualization.

Funding

The author(s) declare that financial support was received for the research and/or publication of this article. NBRC Core funds supported this study. DR was supported by SERB Core Research Grant (CRG) S/SERB/DPR/20230033 extramural grant from the Department of Science and Technology, Ministry of Science and Technology, Govt. India.

Acknowledgments

DR and AB acknowledge the generous support of the NBRC Flagship Program BT/MIDI/NBRC/Flagship/Program/2019: Comparative mapping of common mental disorders (CMD) over the lifespan.

Conflict of interest

The authors declare that the research was conducted in the absence of any commercial or financial relationships that could be construed as a potential conflict of interest.

The author(s) declared that they were an editorial board member of Frontiers, at the time of submission. This had no impact on the peer review process and the final decision.

Generative Al statement

The authors declare that no Generative AI was used in the creation of this manuscript.

Any alternative text (alt text) provided alongside figures in this article has been generated by Frontiers with the support of artificial intelligence and reasonable efforts have been made to ensure accuracy, including review by the authors wherever possible. If you identify any issues, please contact us.

Publisher's note

All claims expressed in this article are solely those of the authors and do not necessarily represent those of their affiliated

organizations, or those of the publisher, the editors and the reviewers. Any product that may be evaluated in this article, or claim that may be made by its manufacturer, is not guaranteed or endorsed by the publisher.

References

Adam, K. C., and Serences, J. T. (2019). Working memory: Flexible but finite. Neuron 103, 184–185. doi: 10.1016/j.neuron.2019.06.025

Baker, S. N. (2007). Oscillatory interactions between sensorimotor cortex and the periphery. *Curr. Opin. Neurobiol.* 17, 649–655. doi: 10.1016/j.conb.2008. 01.007

Benedek, M., Schickel, R. J., Jauk, E., Fink, A., and Neubauer, A. C. (2014). Alpha power increases in right parietal cortex reflects focused internal attention. *Neuropsychologia* 56, 393–400. doi: 10.1016/j.neuropsychologia.2014.02.010

Boettcher, S. E. P., Gresch, D., Nobre, A. C., and van Ede, F. (2021). Output planning at the input stage in visual working memory. $Sci.\ Adv.\ 7$:eabe8212. doi: 10.1126/sciadv. abe8212

Botvinick, M. M., Braver, T. S., Barch, D. M., Carter, C. S., and Cohen, J. D. (2001). Conflict monitoring and cognitive control. *Psychol. Rev.* 108, 624–652. doi: 10.1037/0033-295x.108.3.624

Carlisle, N. B. (2019). Flexibility in attentional control: Multiple sources and suppression. *Yale J. Biol. Med.* 92, 103–113.

Cavanagh, J. F., and Frank, M. J. (2014). Frontal theta as a mechanism for cognitive control. *Trends Cogn. Sci.* 18, 414–421. doi: 10.1111/j.1469-8986.2011. 01293.x

Cavanagh, J. F., and Shackman, A. J. (2015). Frontal midline theta reflects anxiety and cognitive control: Meta-analytic evidence. *J. Physiol.* 109, 3–15. doi: 10.1016/j.jphysparis.2014.04.003

Cavanagh, J. F., Zambrano-Vazquez, L., and Allen, J. J. (2012). Theta lingua franca: A common mid-frontal substrate for action monitoring processes. *Psychophysiology* 49, 220–238. doi: 10.1111/j.1469-8986.2011.01293.x

Chekaf, M., Cowan, N., and Mathy, F. (2016). Chunk formation in immediate memory and how it relates to data compression. *Cognition* 155, 96–107. doi: 10.1016/j.cognition.2016.05.024

Cohen, M. X., and Donner, T. H. (2013). Midfrontal conflict-related theta-band power reflects neural oscillations that predict behavior. *J. Neurophysiol.* 110, 2752–2763. doi: 10.1152/jn.00479.2013

Constant, M., and Liesefeld, H. R. (2021). Massive effects of saliency on information processing in visual working memory. *Psychol. Sci.* 32, 682–691. doi: 10.1177/09567075785

Cowan, N. (1999). "An embedded process model of working memory," in *Models of Working Memory: Mechanisms of Active Maintenance and Executive Control*, eds A. Miyake and P. Shah (Cambridge: Cambridge University Press), 62–101. doi: 10.1017/CBO9781139174909.006

Cowan, N. (2010). The magical mystery four: How is working memory capacity limited, and why? Curr. Dir. Psychol. Sci. 19, 51–57. doi: 10.1177/0963721409359277

Crowder, R. G. (1968). Intraserial repetition effects in immediate memory. J. Verb. Learn. Verb. Behav. 7, 446–451. doi: 10.1016/s0022-5371(68)80031-3

de Vries, I. E., van Driel, J., Karacaoglu, M., and Olivers, C. N. (2018). Priority switches in visual working memory are supported by frontal delta and posterior alpha interactions. *Cereb. Cortex* 28, 4090–4104. doi: 10.1093/cercor/bhy223

Delorme, A., and Makeig, S. (2004). EEGLAB: An open source toolbox for analysis of single-trial EEG dynamics including independent component analysis. *J. Neurosci. Methods* 134, 9–21. doi: 10.1016/j.jneumeth.2003.10.009

Ding, Y., Postle, B. R., and van Ede, F. (2024). Neural signatures of competition between voluntary and involuntary influences over the focus of attention in visual working memory. *J. Cogn. Neurosci.* 36, 815–827. doi: 10.1162/jocn_a_02123

Emrich, S. M., Lockhart, H. A., and Al-Aidroos, N. (2017). Attention mediates the flexible allocation of visual working memory resources. *J. Exp. Psychol. Hum. Percept. Perform.* 43, 1454–1465. doi: 10.1037/xhp0000398

Erickson, M., Smith, D., Albrecht, M., and Silverstein, S. (2019). Alpha-band desynchronization reflects memory-specific processes during visual change detection. *Psychophysiology* 56:e13442. doi: 10.1111/psyp.13442

Faul, F., Erdfelder, E., Lang, A. G., and Buchner, A. (2007). G* Power 3: A flexible statistical power analysis program for the social, behavioral, and biomedical sciences. *Behav. Res. Methods* 39, 175–191. doi: 10.3758/bf03193146

Ferreira, C., Maraver, M., Hanslmayr, S., and Bajo, T. (2019). Theta oscillations show impaired interference detection in older adults during selective memory retrieval. *ScientificReports* 9:9977. doi: 10.1038/s41598-019-46214-8

Greene, R. L. (1991). The Ranschburg effect: The role of guessing strategies. *Memory Cogn.* 19, 313–317. doi: 10.3758/bf03211155

Hamblin-Frohman, Z., Low, J. X., and Becker, S. I. (2023). Attentional prioritisation and facilitation for similar stimuli in visual working memory. *Psychol. Res.* 87, 2031–2038. doi: 10.1007/s00426-023-01790-3

Ichihara-Takeda, S., Yazawa, S., Murahara, T., Toyoshima, T., Shinozaki, J., Ishiguro, M., et al. (2015). Modulation of alpha activity in the parieto-occipital area by distractors during a visuospatial working memory task: A magnetoencephalographic study. *J. Cogn. Neurosci.* 27, 453–463. doi: 10.1162/jocn_a_00718

Jacobs, J., Hwang, G., Curran, T., and Kahana, M. (2006). EEG oscillations and recognition memory: Theta correlates of memory retrieval and decision making. *Neuroimage* 32, 978–987. doi: 10.1016/j.neuroimage.2006.02.018

Johnson, E. L., Dewar, C. D., Solbakk, A. K., Endestad, T., Meling, T. R., and Knight, R. T. (2017). Bidirectional frontoparietal oscillatory systems support working memory. *Curr. Biol.* 27, 1829–1835.e4. doi: 10.1016/j.cub.2017.05.046

Kaiser, J., Iliopoulos, P., Steinmassl, K., and Schütz-Bosbach, S. (2022). Preparing for success: Neural frontal theta and posterior alpha dynamics during action preparation predict flexible resolution of cognitive conflicts. *J. Cogn. Neurosci.* 34, 1070–1089. doi: 10.1162/jocn_a_01846

Kilavik, B. E., Zaepffel, M., Brovelli, A., MacKay, W. A., and Riehle, A. (2013). The ups and downs of beta oscillations in sensorimotor cortex. *Exp. Neurol.* 245, 15–26. doi: 10.1016/j.expneurol.2012.09.014

Klimesch, W. (1999). EEG alpha and theta oscillations reflect cognitive and memory performance: A review and analysis. *Brain Res. Rev.* 29, 169–195. doi: 10.1016/s0165-0173(98)00056-3

Larocque, J. J., Lewis-Peacock, J. A., and Postle, B. R. (2014). Multiple neural states of representation in short-term memory? It's a matter of attention. *Front. Hum. Neurosci.* 8:5. doi: 10.3389/fnhum.2014.00005

Lee, C. L. (1976). Short-term recall of repeated items and detection of repetitions in letter sequences. *J. Exp. Psychol. Hum. Learn. Mem.* 2, 120–127. doi: 10.1037//0278-7393.2.2.120

Li, Z., Zhang, J., Liang, T., Ye, C., and Liu, Q. (2020). Interval between two sequential arrays determines their storage state in visual working memory. *Sci. Rep.* 10:7706. doi: 10.1038/s41598-020-64825-4

Li, Z., Liang, T., and Liu, Q. (2021). The storage resources of the active and passive states are independent in visual working memory. *Cognition* 217:104911. doi: 10.1016/j.cognition.2021.104911

Lin, P.-H., and Luck, S. J. (2009). The influence of similarity on visual working memory representations. *Vis. Cogn.* 17, 356–372. doi: 10.1080/13506280701766313

Magosso, E., and Borra, D. (2024). The strength of anticipated distractors shapes EEG alpha and theta oscillations in a working memory task. Neuroimage~300:120835. doi: 10.1016/j.neuroimage.2024.120835

Makeig, S. (1993). Auditory event-related dynamics of the EEG spectrum and effects of exposure to tones. *Electroencephalogr. Clin. Neurophysiol.* 86, 283–293. doi: 10.1016/0013-4694(93)90110-h

Maris, E., and Oostenveld, R. (2007). Nonparametric statistical testing of EEG-and MEG-data. J. Neurosci. Methods 164, 177–190. doi: 10.1016/j.jneumeth.2007.03.024

McFarland, D. J., Miner, L. A., Vaughan, T. M., and Wolpaw, J. R. (2000). Mu and beta rhythm topographies during motor imagery and actual movements. Brain Topogr. 12, 177–186. doi: 10.1023/a:1023437823106

Miller, G. A. (1956). The magical number seven, plus or minus two: Some limits on our capacity for processing information. *Psychol. Rev.* 63:81. doi: 10.1037/0033-295x. 101.2.343

Nasrawi, R., and van Ede, F. (2022). Planning the potential future during multi-item visual working memory. *J. Cogn. Neurosci.* 34, 1534–1546. doi: 10.1162/jocn_a_01875

Nasrawi, R., Boettcher, S. E., and van Ede, F. (2023). Prospection of potential actions during visual working memory starts early, is flexible, and predicts behavior. *J. Neurosci.* 43, 8515–8524. doi: 10.1523/JNEUROSCI.0709-23.2023

Neuper, C., Wörtz, M., and Pfurtscheller, G. (2006). ERD/ERS patterns reflecting sensorimotor activation and deactivation. *Prog. Brain Res.* 159, 211–222. doi: 10.1016/S0079-6123(06)59014-4

Nigbur, R., Ivanova, G., and Stürmer, B. (2011). Theta power as a marker for cognitive interference. *Clin. Neurophysiol.* 122, 2185–2194. doi: 10.1016/j.clinph.2011. 03.030

Oberauer, K. (2002). Access to information in working memory: Exploring the focus of attention. *J. Exp. Psychol. Learn. Mem. Cogn.* 28:411. doi: 10.1037/0278-7393.28.3.411

Oberauer, K., and Lange, E. B. (2009). Activation and binding in verbal working memory: A dual-process model for the recognition of nonwords. *Cogn. Psychol.* 58, 102–136. doi: 10.1016/j.cogpsych.2008.05.003

Olivers, C. N., Peters, J., Houtkamp, R., and Roelfsema, P. R. (2011). Different states in visual working memory: When it guides attention and when it does not. *Trends Cogn. Sci.* 15, 327–334. doi: 10.1016/j.tics.2011.05.004

Onton, J., Delorme, A., and Makeig, S. (2005). Frontal midline EEG dynamics during working memory. *Neuroimage* 27, 341–356. doi: 10.1016/j.neuroimage.2005. 04.014

Peters, J. C., Goebel, R., and Roelfsema, P. R. (2009). Remembered but unused: The accessory items in working memory that do not guide attention. *J. Cogn. Neurosci.* 21, 1081–1091. doi: 10.1162/jocn.2009.21083

Peterson, D., and Berryhill, M. (2013). The Gestalt principle of similarity benefits visual working memory. *Psychon. Bull. Rev.* 20, 1282–1289. doi: 10.3758/s13423-013-0460-x

Pfurtscheller, G., and Da Silva, F. L. (1999). Event-related EEG/MEG synchronization and desynchronization: Basic principles. *Clin. Neurophysiol.* 110, 1842–1857. doi: 10.1016/s1388-2457(99)00141-8

Ren, G., Ma, N., and Lei, M. (2023). The facilitating effect of identical objects in visual working memory. *Front. Psychol.* 13:1092557. doi: 10.3389/fpsyg.2022.1092557

Riddle, J., Scimeca, J. M., Cellier, D., Dhanani, S., and D'Esposito, M. (2020). Causal evidence for a role of theta and alpha oscillations in the control of working memory. *Curr. Biol.* 30, 1748–1754. doi: 10.1016/j.cub.2020.02.065

Sauseng, P., and Liesefeld, H. R. (2020). Cognitive control: Brain oscillations coordinate human working memory. *Curr. Biol.* 30, R405–R407. doi: 10.1016/j.cub. 2020.02.067

Sauseng, P., Griesmayr, B., Freunberger, R., and Klimesch, W. (2010). Control mechanisms in working memory: A possible function of EEG theta oscillations. *Neurosci. Biobehav. Rev.* 34, 1015–1022. doi: 10.1016/j.neubiorev.2009.12.006

Sauseng, P., Klimesch, W., Stadler, W., Schabus, M., Doppelmayr, M., Hanslmayr, S., et al. (2005). A shift of visual spatial attention is selectively associated with human

EEG alpha activity. Eur. J. Neurosci. 22, 2917–2926. doi: 10.1111/j.1460-9568.2005. 04482.x

Schneider, D., Barth, A., and Wascher, E. (2017). On the contribution of motor planning to the retroactive cuing benefit in working memory: Evidence by mu and beta oscillatory activity in the EEG. *Neuroimage* 162, 73–85. doi: 10.1016/j.neuroimage. 2017.08.057

Thalmann, M., Souza, A. S., and Oberauer, K. (2019). How does chunking help working memory? *J. Exp. Psychol. Learn. Mem. Cogn.* 45:37. doi: 10.1037/xlm0000578

Theeuwes, J. (1992). Perceptual selectivity for color and form. *Percept. Psychophys.* 51, 599–606, doi: 10.3758/bf03211656

van Ede, F., Niklaus, M., and Nobre, A. C. (2017). Temporal expectations guide dynamic prioritization in visual working memory through attenuated α oscillations. *J. Neurosci.* 37, 437–445. doi: 10.1523/JNEUROSCI.2272-16.

van Moorselaar, D., Theeuwes, J., and Olivers, C. (2014). In competition for the attentional template: Can multiple items within visual working memory guide attention? *J. Exp. Psychol. Hum. Percept. Perform.* 40, 1450–1464. doi: 10.1037/a0036229

Van Wijk, B. C. M., Daffertshofer, A., Roach, N., and Praamstra, P. (2009). A role of beta oscillatory synchrony in biasing response competition? *Cereb. Cortex* 19, 1294–1302. doi: 10.1093/cercor/bhn174

Wickham, H. (2011). Ggplot2. Wiley Interdiscip. Rev. Comput. Stat. 3, 180–185. doi:10.1002/wics.147

Wolfe, J. M. (1994). Guided Search 2.0 A revised model of visual search. *Psychonom. Bull. Rev.* 1, 202–238. doi: 10.3758/BF03200774

Woodman, G. F., Luck, S. J., and Schall, J. D. (2007). The role of working memory representations in the control of attention. $Cereb.\ Cortex\ 17, i118-i124.\ doi:\ 10.1093/cercor/bhm065$

Zhang, J., Ye, C., Sun, H.-J., Zhou, J., Liang, T., Li, Y., et al. (2022). The passive state: A protective mechanism for information in working memory tasks. *J. Exp. Psychol. Learn. Mem. Cogn.* 48, 1235–1248. doi: 10.1037/xlm0001092

Zuure, M. B., Hinkley, L. B., Tiesinga, P. H. E., Nagarajan, S. S., and Cohen, M. X. (2020). Multiple midfrontal thetas revealed by source separation of simultaneous MEG and EEG. *J. Neurosci.* 40, 7702–7713. doi: 10.1523/JNEUROSCI.0321-20.2020